Negative-differential band-gap renormalization in type-II GaAs/AlAs superlattices

W. Langbein, S. Hallstein, and H. Kalt
Institut für Angewandte Physik, Universität Karlsruhe, D-76128 Karlsruhe, Germany

R. Nötzel and K. Ploog
Paul-Drude-Institut für Festkörperphysik, D-10117 Berlin, Germany
(Received 22 September 1994)

We report on a quantitative determination of the band-gap renormalization in type-II GaAs/AlAs superlattices under high excitation. The time-resolved luminescence after picosecond high excitation is analyzed using a detailed luminescence line-shape fit. We find the renormalization of the type-I transition to be comparable to that in type-I superlattices, whereas the type-II transition reveals a negative-differential renormalization. This is attributed to the space-charge effects caused by the carrier separation in agreement with quantitative calculations.

The nonlinear optical properties of type-II superlattices (SL's) have attracted much research work in the last few years. The GaAs/AlAs system with narrow GaAs layers, where the lowest conduction-band state is confined in the AlAs layers, is useful as a model type-II system due to the well-known properties of the corresponding type-I SL's and the perfection of the growth technology. The lowest transition in this system is indirect both in real and reciprocal space,[1,2] leading to a carrier recombination time in the microsecond regime and thus permitting high carrier densities even under cw excitation.[3] The nonlinear properties of this system[4,5] reveal the influence of the space-charge field on the transition energies and the ultrafast optical nonlinearity at the direct band edge due to the subpicosecond Γ-X transfer time.[6,7]

We report here on a quantitative study of the band-gap renormalization (BGR) in such type-II SL's, which is strongly influenced by the space-charge fields. The investigations were performed on several type-II GaAs/AlAs superlattices having different layer thicknesses and correspondingly different Γ-X splittings. We use the time-resolved luminescence after picosecond high excitation to analyze the BGR using a detailed luminescence line-shape calculation accounting for several conduction- and valence-band subbands, subband dispersions, energy-dependent transition strengths of the type-II transition, and collision broadening. As a function of carrier density, we find a blueshift of the type-II subband energy, while the type-I subband gap narrows similar as in a type-I SL.

We present here the quantitative results for the sample with the largest Γ-X splitting, revealing the best distinctions between the Γ and the X luminescence. The sample was grown by molecular beam epitaxy (MBE) on a (100) GaAs substrate and consists of 140 periods of 2.3-nm GaAs and 2.2-nm AlAs, characterized by high resolution x-ray diffraction. The low-excitation photoluminescence (PL) and photoluminescence excitation (PLE) spectra (Fig. 1) were recorded at 10 K with a tungsten lamp dispersed by a monochromator as the excitation source. The PL of the SL shows a zero-phonon line and two weak phonon replica, which can be attributed to the TA and LO AlAs phonon transition.[2] The PLE reveals the type-II configuration of the sample. The time-resolved high-excitation luminescence of the sample was recorded at a lattice temperature of 5 K after excitation by intense 70-ps pulses at 2.46 eV. The temporal and spectral dispersion was achieved using a sequence of a spectrometer and a streak camera.

The normalized time-resolved luminescence for different initial densities and delay times is shown in Fig. 2. One can nicely follow the whole density dependence of the luminescence. At low densities, only the type-II X_z-hh (heavy hole) luminescence is present, broadening with density. With increasing density, the type-I Γ-hh luminescence takes over. At very high densities exceeding 10^{13} cm^{-2} one can additionally observe the transition to the light hole. These assignments of the different luminescence bands are supported by their decay times and by the subsequent theoretical analysis.

A quantitative determination of the band-gap renormalization of the different subbands out of the time-resolved luminescence data is achieved by its comparison with theoretical calculations of the luminescence line shape accounting for the population of different electron

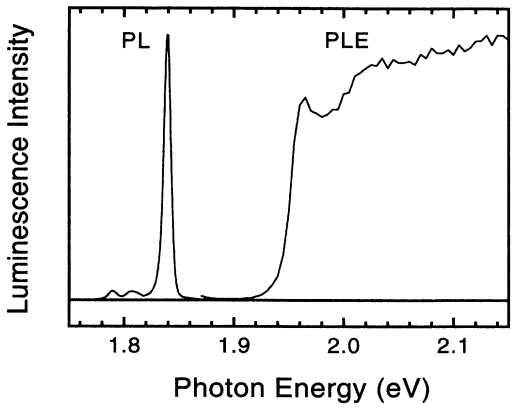

FIG. 1. Photoluminescence (PL) and photoluminescence excitation (PLE) spectra of the investigated type-II GaAs/AlAs SL.

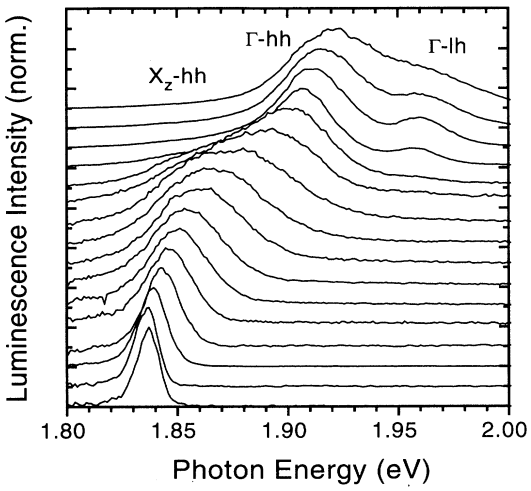

FIG. 2. Dynamics of the high-excitation luminescence of the type-II GaAs/AlAs SL various excitation intensities and delay times (from the top to the bottom: 2.5 mJ/cm^2 at 100 ps, 150 ps, 250 ps, 500 ps, 1 ns, 1.5 ns, 2.4 ns, 3.4 ns, 5 ns, 8 ns, 11 ns, 20 ns; 250 μJ/cm^2 at 15 ns; 62 μJ/cm^2 at 3 ns; 15 μJ/cm^2 at 2 ns, 65 ns).

and hole subbands. The miniband structure of these subbands is computed using a Kronig-Penney model. The resulting miniband dispersions for the investigated sample (Fig. 3) show miniband widths that are small for the first X_z and for the first hh miniband. The first Γ and $X_{x,y}$ minibands have widths of about 20 meV and 40 meV, respectively, which significantly changes the density of states compared to the uncoupled case. The recombination between electron and hole subbands is calculated respecting momentum conservation and including a phenomenological state broadening due to many-particle interactions in the plasma.[8] The type-I transition is direct in momentum space and the wave-function overlap is approximately one, leading to an energy-independent transition strength and the luminescence is given by

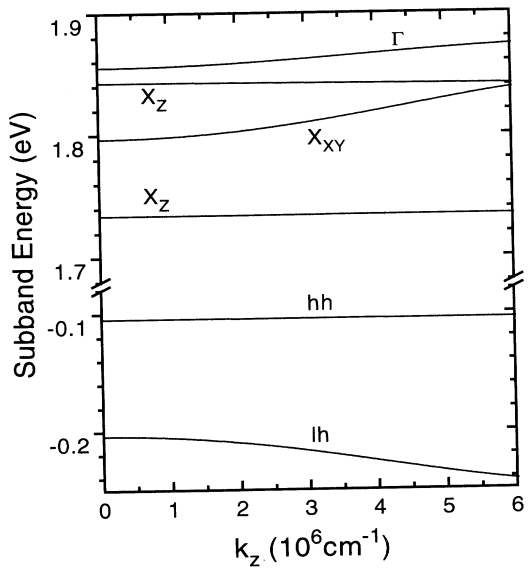

FIG. 3. Miniband dispersion of the type-II GaAs/AlAs SL for the lowest state of the Γ, X_z, hh and lh (light hole) bands using a Kronig-Penney calculation.

$$I_\Gamma(\hbar\omega) \propto \sum_{ij}^{\text{subbands}} a_{ij}^\Gamma \int_{-\infty}^{\infty} d^2k_\parallel \int_{-\pi/d}^{\pi/d} dk_z \int_{-\infty}^{\infty} dE_e \times A_i^e(k_\parallel, k_z, E_e) f_e(E_e) \int_{-\infty}^{\infty} dE_h \times A_j^h(k_\parallel, k_z, E_h) f_h(E_h) \delta(\hbar\omega - E_e - E_h) \quad (1)$$

with

$$A_{i,j}^{e,h}(k_\parallel, k_z, E_{e,h}) = \gamma_{i,j}(E_{e,h} - E_{i,j}^{e,h}(k\|, k_z))$$

and

$$\gamma_{i,j}(x) = \begin{cases} \frac{1}{N_{i,j}} \frac{\Gamma_{i,j}}{x^2+\Gamma_{i,j}^2}, & -\frac{3}{2}\hbar\omega_{\text{pl}} < x < \hbar\omega_{\text{pl}} \\ 0, & \text{else.} \end{cases}$$

Here, a_{ij}^Γ is the transition probability between the Γ conduction miniband i and the valence miniband j, given by the dipole matrix element and the overlap integral. The state broadening $A^{e,h}$ is of Lorenzian-type, cut off at the plasma frequency $\hbar\omega_{\text{pl}}$.[9] The Fermi distributions $f_{e,h}$ are given by the carrier temperature and density, $E^{e,h}$ are the miniband and in-plane dispersions of the different subbands, and d is the SL period.

The type-II zero-phonon transition, which is dominant over the phonon-assisted processes (see Fig. 1), complies with the momentum conservation in spite of the fact that it is indirect in momentum space. This is because the superlattice potential, which is responsible for the X_z-Γ intermixture, inherits only momentum components in the growth direction **z** at the zone edge of the mini-Brillouin zone, thus conserving the in-plane momentum $k_\parallel$ and the miniband momentum k_z. The strength of this transition is given by the intermixing and the wave-function overlap. The overlap is independent of the in-plane wave vector as long as one neglects the nonparabolicity of the bands. The intermixing is given in first-order perturbation theory by[10,11]

$$I \propto \left(\frac{|\langle \Psi_\Gamma | V_{\Gamma X} | \Psi_X \rangle|}{E_\Gamma(k_\parallel, k_z) - E_X(k_\parallel, k_z)} \right)^2 \quad (2)$$

with the Γ-X mixing potential $V_{\Gamma X}$. We, therefore, get a dependence of the transition strength on $k_\parallel$ and k_z, which is included in the calculation for the indirect luminescence

$$I_X(\hbar\omega) \propto \sum_{ij}^{\text{subbands}} a_{ij}^X \int_{-\infty}^{\infty} d^2k_\parallel \int_{-\pi/d}^{\pi/d} dk_z \times \int_{-\infty}^{\infty} dE_e A_i^e f_e \int_{-\infty}^{\infty} dE_h A_j^h f_h \times \frac{D_{\Gamma X} \delta(\hbar\omega - E_e - E_h)}{(E_{\text{min}}^\Gamma - E_e)^2 + D_{\Gamma X}^2} . \quad (3)$$

Here, the exchange energy $D_{\Gamma X}$ accounts for the noncrossing of the two states, but is of minor importance

in this case due to the bigger in-plane mass of the X_z subband compared to the Γ subband, thus prohibiting a state crossing of the in-plane dispersions. The transition strength is represented by a_{ij}^X. The luminescence from the $X_{x,y}$ subbands can be neglected because of the diminutive transition strength[1] of the phonon-assisted and the interface-roughness induced transitions.

We retrieve the band-gap energies, the carrier temperature, the carrier density, and the state broadening by a fit of the calculated to the experimental luminescence lineshape. In this procedure, we take the transition strengths between heavy and light hole to be[12] 3:1. The relative oscillator strength of Γ and X excitons was estimated in Ref. 10 to be of the order of 10^4:1, but the authors do not use the combined density of states in their calculation and they neglect miniband effects on the Γ exciton. In our model we found the relative transition strength between Γ and X to be 100:1. These values are held constant for all fits to the luminescence of this sample.

In Fig. 4 the experimental and the calculated luminescence line shape with the corresponding parameters for three prominent excitation densities are plotted. At 4.5×10^{11} cm^{-2} (a) only the X_z conduction band and the hh valence band are occupied. Below this density, we observe a turnover from plasma to exciton luminescence, which is evident from the luminescence linewidth. At 5.3×10^{12} cm^{-2} (b) the Γ conduction band gets occupied and takes over the major luminescence component due to its much higher transition strength. At 9.8×10^{12} cm^{-2} (c) all three conduction bands and the two valence bands are occupied and one can distinguish at least three different contributions to the total luminescence, denoted by the corresponding transitions.

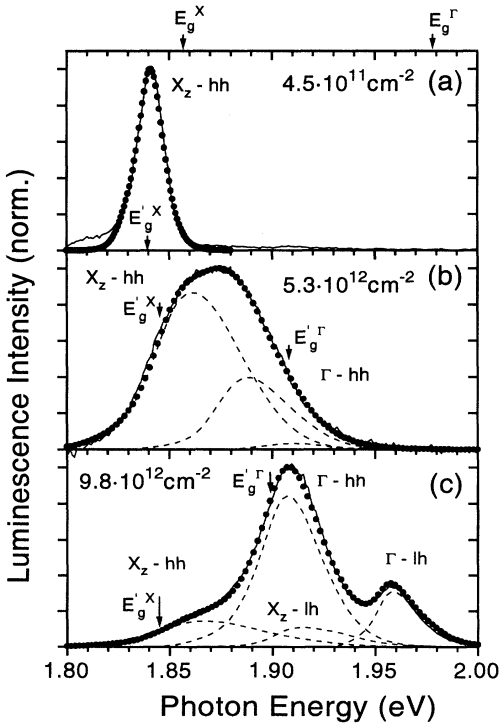

FIG. 4. Line-shape fits (dots) to the experimental luminescence spectra at different excitation densities. The dashed lines are the different contributions to the luminescence, the arrows indicate the renormalized (E'_g) and unrenormalized (E_g) subband gaps.

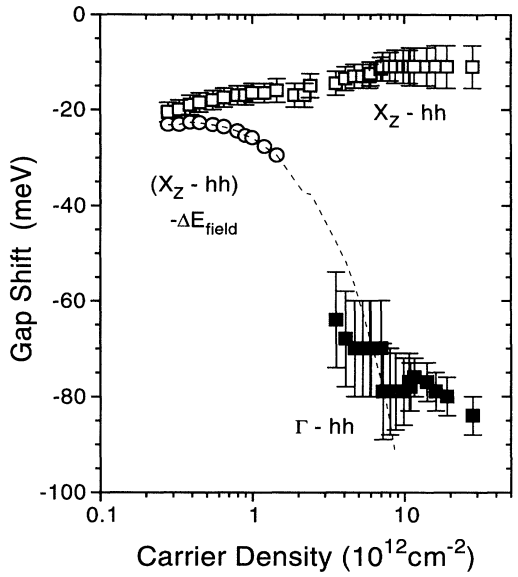

FIG. 5. Experimental density dependence of the type-I and type-II transition band gaps in the SL. The dashed line represents the contribution of the exchange and correlation effects to the type-II band-gap shift.

The band-gap energies deduced from the fit are subtracted from the subband-gap energies at low excitation as determined by PL and PLE spectra (Fig. 1), leading to the absolute subband-gap shift (Fig. 5). The two transitions reveal a quite different renormalization. The type-I Γ1-hh1 transition exhibits a strong renormalization with increasing density, typical for type-I transitions[13] due to the dominating exchange and correlation effects. The type-II X_z1-hh1 transition shows only a weak absolute renormalization with a negative differential slope. This is caused by the band-structure modifications induced by space-charge effects. The resulting density-dependent increase of the type-II subband gap is larger than the reduction evoked by the exchange and correlation effects. Our experimental results are in qualitative agreement with the calculation by Havrylak,[14] a quantitative comparison with his results is not meaningful because of the incomparable period length.

Nevertheless, the space-charge effects can be easily estimated assuming sine-wave functions in the GaAs layer for the holes and in the AlAs-layer for the electrons, leading to a transition energy shift according to

$$\Delta E = \frac{e^2 n_{2D}}{\epsilon \epsilon_0} d \left(\frac{1}{12} + \frac{1}{2\pi^2} \right) \tag{4}$$

with the in-plane carrier density n_{2D}, the dielectric constant ϵ, and the period length d. For the investigated SL this results in a shift of 9.3 meV/10^{12} cm^{-2}. To compare

the correlation and exchange energies in both transitions, we have subtracted the electrostatic shift from the X_z-hh transition energy according to this formula (Fig. 5). This is only valid as long as only the lowest X_z conduction band is occupied, as marked with symbols. At higher densities the space-charge effects are overestimated due to the extent of the now occupied $X_{x,y}$ and Γ subbands in the GaAs layer. The remaining exchange and correlation energies in the type-II transition are comparable to those of the type-I transition, which is nearly uneffected by the space-charge effects.

In conclusion, we have quantitatively determined the influence of the space-charge effects on the renormalization of type-II SL's, leading to a negative-differential BGR of the type-II transitions, whereas the type-I transitions show the same behavior as in type-I SL's.

[1] G. Danan, B. Etienne, F. Mollot, R. Planel, A.M. Jean-Louis, F. Alexandre, B. Jusserand, G. Le Roux, J.Y. Marzin, H. Savary, and B. Sermage, Phys. Rev. B **35**, 6207 (1987).

[2] H.W. Kesteren, E.C. Cosman, P. Dawson, K.J. Moore, and C.T. Foxon, Phys. Rev. B **39**, 13 426 (1989).

[3] J.F. Angell and M.D. Sturge, Phys. Rev. B **48**, 4650 (1993).

[4] R. Binder, I. Galbraith, and S.W. Koch, Phys. Rev. B **44**, 3301 (1991).

[5] G.R. Olbright, W.S. Fu, J.F. Klem, H.M. Gibbs, G. Khitrova, R. Pon, B. Fluegel, K. Meissner, N. Peyghambarian, R. Binder, I. Galbraith, and S.W. Koch, Phys. Rev. B **44**, 3043 (1991).

[6] J. Feldmann, R. Sattmann, E.O. Göbel, J. Kuhl, J. Hebling, K. Ploog, R. Muralidharan, P. Dawson, and C.T. Foxon, Phys. Rev. Lett. **62**, 1892 (1989).

[7] B. Deveaud, F. Clérot, A. Regreny, R. Planel, and J.M. Gérard, Phys. Rev. B **49**, 13 560 (1994).

[8] G. Bongiovanni and J.L. Staehli, Phys. Rev. B **39**, 8359 (1989), and references therein.

[9] A. Selloni, S. Modesti, M. Capizzi, Phys. Rev. B **30**, 821 (1984).

[10] M. Nakayama K. Imazawa, K. Suyama, I. Tanaka, and H. Nishimura, Phys. Rev. B **49**, 13 564 (1994).

[11] T. Ando, Phys. Rev. B **47**, 9621 (1993).

[12] E.O. Goebel and K. Ploog, Prog. Quantum Electron. **14**, 289 (1990).

[13] G. Tränkle, E. Lach, A. Forchel, F. Scholz, C. Ell, H. Haug, G. Weimann, G. Griffiths, H. Kroemer, and S. Subbanna, Phys. Rev. B **36**, 6712 (1987).

[14] P. Havrylak, Phys. Rev. B **39**, 6264 (1989).